J|A|C|S ARTICLES

Published on Web 10/26/2009

Characterization of the SgcF Epoxide Hydrolase Supporting an (*R*)-Vicinal Diol Intermediate for Enediyne Antitumor Antibiotic C-1027 Biosynthesis

Shuangjun Lin,[†] Geoffrey P. Horsman,[†] Yihua Chen,[†] Wenli Li,[†] and Ben Shen*[,†,‡,§]

Division of Pharmaceutical Sciences, University of Wisconsin National Cooperative Drug Discovery Group, and Department of Chemistry, University of Wisconsin-Madison, Madison, Wisconsin 53705-2222

Received February 17, 2009; E-mail: bshen@pharmacy.wisc.edu

Abstract: C-1027 is a chromoprotein antitumor antibiotic consisting of an apoprotein and the C-1027 chromophore. The C-1027 chromophore possesses four distinct structural moieties—an enediyne core, a deoxy aminosugar, a benzoxazolinate, and an (*S*)-3-chloro-5-hydroxy-β-tyrosine—the latter two of which are proposed to be appended to the enediyne core via a convergent biosynthetic strategy. Here we report the in vitro characterization of SgcF, an epoxide hydrolase from the C-1027 biosynthetic gene cluster that catalyzes regio- and stereospecific hydrolysis of styrene oxide, serving as an enediyne core epoxide intermediate mimic, to form a vicinal diol. Abolishment of C-1027 production in the Δ*sgcF* mutant strain *Streptomyces globisporus* SB1010 unambiguously establishes that *sgcF* plays an indispensable role in C-1027 biosynthesis. SgcF efficiently hydrolyzes (*S*)-styrene oxide, displaying an apparent K_m of 0.6 ± 0.1 mM and k_{cat} of 48 ± 1 min^{-1}, via attack at the α-position to exclusively generate the (*R*)-phenyl vicinal diol, consistent with the stereochemistry of the C-1027 chromophore. These findings support the role of SgcF in the proposed convergent pathway for C-1027 biosynthesis, unveiling an (*R*)-vicinal diol as a key intermediate. Interestingly, SgcF can also hydrolyze (*R*)-styrene oxide to afford preferentially the (*R*)-phenyl vicinal diol via attack at the β-position, albeit with significantly reduced efficiency (apparent K_m of 2.0 ± 0.4 mM and k_{cat} = 4.3 ± 0.3 min^{-1}). Although the latter activity unlikely contributes to C-1027 biosynthesis in vivo, such enantioconvergence arising from complementary regioselective hydrolysis of a racemic substrate could be exploited to engineer epoxide hydrolases with improved regio- and/or enantiospecificity.

Introduction

The enediynes are some of the most cytotoxic molecules known to date, and two members of this family, calicheamicin and neocarzinostatin (NCS), are currently in clinical use as anticancer drugs.[1,2] The enediyne cores of molecules such as C-1027 and NCS possess multiple vicinal diols (Figure 1), to which the various peripheral moieties are attached to impart the distinct characteristics of each enediyne antitumor antibiotic. These functional groups may be envisaged to originate from epoxide precursors that undergo hydrolytic ring-opening catalyzed by epoxide hydrolases (EHs).

The ubiquity of EHs in nature is evidenced by their widespread occurrence in mammals, plants, insects, and various microorganisms such as yeast, fungi, and bacteria.[3−6] Most EHs belong to the α/β-hydrolase superfamily,[7−9] and crystallographic studies have confirmed the presence of this structural fold in several EHs.[10−17] Detailed analysis of available sequence and structural data has revealed that EHs possess a modular

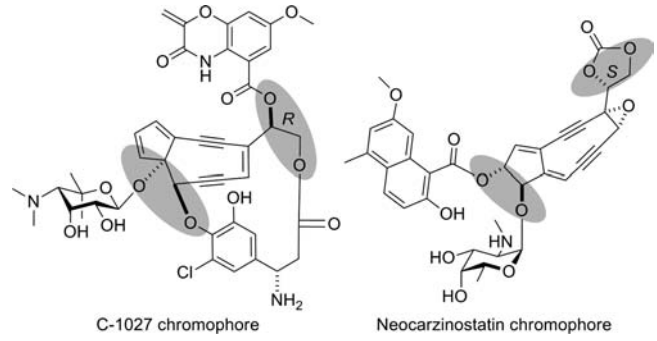

Figure 1. Structures of C-1027 and neocarzinostatin, with vicinal diol moieties (shaded) predicted to be derived by epoxide hydrolases from enediyne core epoxide precursors.

[†] Division of Pharmaceutical Sciences.
[‡] University of Wisconsin National Cooperative Drug Discovery Group.
[§] Department of Chemistry.

(1) Shen, B.; Liu, W.; Nonaka, K. *Curr. Med. Chem.* **2003**, *10*, 2317–2325.
(2) Van Lanen, S. G.; Shen, B. *Curr. Top. Med. Chem.* **2008**, *8*, 448–459.
(3) Archelas, A.; Furstoss, R. *Curr. Opin. Chem. Biol.* **2001**, *5*, 112–119.
(4) Lee, E. Y.; Shuler, M. L. *Biotechnol. Bioeng.* **2007**, *98*, 318–327.
(5) Steinreiber, A.; Faber, K. *Curr. Opin. Biotechnol.* **2001**, *12*, 552–558.
(6) Weijers, C. A. G. M; de Bont, J. A. M. *J. Mol. Catal. B: Enzym.* **1999**, *6*, 199–214.
(7) Heikinheimo, P.; Goldman, A.; Jeffries, C.; Ollis, D. L. *Structure* **1999**, *7*, 141–146.
(8) Holmquist, M. *Curr. Prot. Pept. Sci.* **2000**, *1*, 209–235.
(9) Ollis, D. L.; Cheah, E.; Cygler, M.; Dijkstra, B.; Frolow, F.; Franken, S. M.; Harel, M.; Remington, S. J.; Silman, I.; Schrag, J.; Sussman, J. L.; Verscheuren, K. H. G.; Goldman, A. *Protein Eng.* **1992**, *5*, 197–211.

10.1021/ja901242s CCC: $40.75

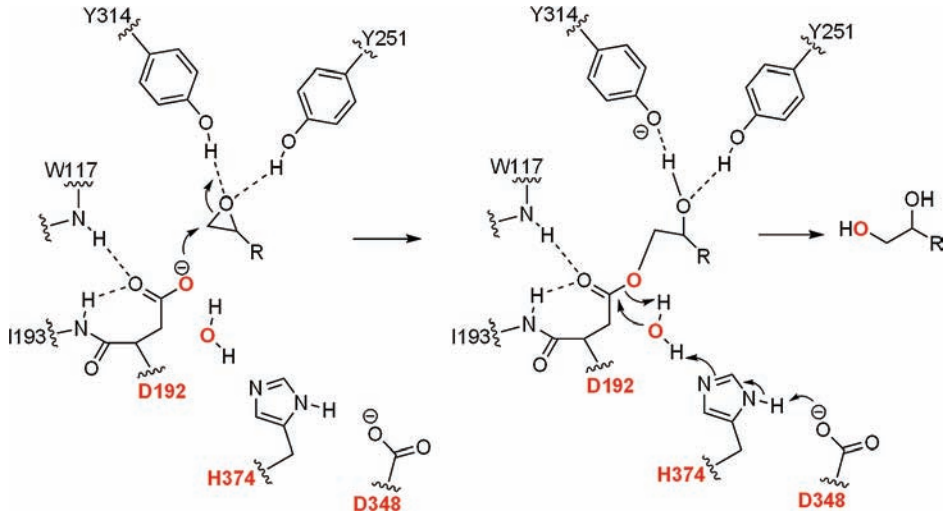

Figure 2. Proposed mechanism of epoxide hydrolases. The catalytic triad and the oxygen atom from water are shown in red, and the active site residues reflect those of AnEH from *Aspergillus niger*.[17]

architecture consisting of three conserved and three variable regions (Figure S1, Supporting Information).[18,19] The conserved regions include the N- and C-terminal catalytic regions that together make up the core catalytic domain of the α/β-hydrolase fold, as well as the lid or cap domain. The variable regions include: (i) an N-terminal region that may include a membrane anchor or may be missing altogether as in most bacterial EHs; (ii) an NC-loop linking the lid and the N-terminal catalytic domain; and (iii) a variable loop in the lid domain (cap-loop). The active site is located at the interface between the core and lid domains and contains five residues that are absolutely conserved among EHs − the nucleophile (Asp or Glu) and His of the nucleophile-His-acid triad (the acid residue of which is variable in its position), the 2 residues of the oxyanion hole (X of the HGXP motif, and the residue following the catalytic nucleophile), and a conserved Tyr in the fifth helix of the lid domain (i.e., α8 in Figure S2, Supporting Information). Although most EHs possess a second Tyr in the first helix of the lid domain (i.e., α4 in Figure S2, Supporting Information), this residue is not always conserved.[19]

The conserved structure and active site residues reflect a common mechanism for epoxide hydrolysis (Figure 2). The two tyrosine residues in the lid domain form hydrogen bonds to the oxirane oxygen atom,[10,20−22] thereby activating the epoxide to be attacked by the nucleophilic Asp/Glu residue of the catalytic triad to yield a covalent alkyl-enzyme intermediate.[23−25] A water molecule, activated by a conserved His-Asp charge relay system, hydrolyzes the monoester intermediate to afford the vicinal diol as a product. The transient oxyanion tetrahedral intermediate is stabilized via hydrogen bonds to the backbone amide hydrogens of the oxyanion hole residues.[15−17,26]

Although mammalian EHs have been studied for decades for their roles in xenobiotic detoxification[27,28] and other physiological functions,[29] microbial EHs have recently become attractive for biocatalytic applications due to their regio- and enantioselectivity and solubility,[3,4,30,31] and little is known about their roles in natural product biosynthesis. For an asymmetric epoxide such as styrene oxide, microbial EHs with various regio- and enantioselectivity have been reported. Most microbial EHs preferentially hydrolyze one enantiomer of an epoxide racemate, and thereby may be utilized to generate enantiopure epoxides or diols via kinetic resolution. Interestingly, a few EHs have been reported to catalyze the hydrolysis of both enantiomers to form enantiomerically enriched diol products.[32] This enantioconvergent process occurs by means of complementary enantio-

(10) Argiriadi, M. A.; Morisseau, C.; Goodrow, M. H.; Dowdy, D. L.; Hammock, B. D.; Christianson, D. W. *J. Biol. Chem.* **2000**, *275*, 15265–15270.
(11) Argiriadi, M. A.; Morisseau, C.; Hammock, B. D.; Christianson, D. W *Proc. Natl. Acad. Sci. U.S.A.* **1999**, *96*, 10637–10642.
(12) Gomez, G. A.; Morisseau, C.; Hammock, B. D.; Christianson, D. W. *Biochemistry* **2004**, *43*, 4716–4723.
(13) Gomez, G. A.; Morisseau, C.; Hammock, B. D.; Christianson, D. W. *Protein Sci.* **2006**, *15*, 58–64.
(14) Mowbray, S. L.; Elfstrom, L. T.; Ahlgren, K. M.; Andersson, C. E.; Widersten, M. *Protein Sci.* **2006**, *15*, 1628–1637.
(15) Nardini, M.; Rick, R. B.; Janssen, D. B.; Dijkstra, B. W. *J. Mol. Catal. B: Enzym.* **2001**, *11*, 1035–1042.
(16) Nardini, M.; Ridder, I. S.; Rozeboom, H. J.; Kalk, K. H.; Rink, R.; Janssen, D. B.; Dijkstra, B. W. *J. Biol. Chem.* **1999**, *274*, 14579–14586.
(17) Zou, J. Y.; Hallberg, B. M.; Bergfors, T.; Oesch, F.; Arand, M.; Mowbray, S. L.; Jones, T. A. *Structure* **2000**, *8*, 111–122.
(18) Barth, S.; Fischer, M.; Schmid, R. D.; Pleiss, J. *Bioinformatics* **2004**, *20*, 2845–2847.
(19) Barth, S.; Fischer, M.; Schmid, R. D.; Pleiss, J. *Proteins: Struct. Funct. Bioinform.* **2004**, *55*, 846–855.
(20) Rink, R.; Kingma, J.; Spelberg, J. H. L.; Janssen, D. B. *Biochemistry* **2000**, *39*, 5600–5613.
(21) Rink, R.; Spelberg, J. H. L.; Pieters, R. J.; Kingma, J.; Nardini, M.; Kellogg, R. M.; Dijkstra, B. W.; Janssen, D. B. *J. Am. Chem. Soc.* **1999**, *121*, 7417–7418.
(22) Yamada, T.; Morisseau, C.; Maxwell, J. E.; Argiriadi, M. A.; Christianson, D. W.; Hammock, B. D. *J. Biol. Chem.* **2000**, *275*, 23082–23088.
(23) Hammock, B. D.; Pinot, F.; Beetham, J. K.; Grant, D. F.; Arand, M. E.; Oesch, F. *Biochem. Biophys. Res. Commun.* **1994**, *198*, 850–856.
(24) Lacourciere, G. M.; Armstrong, R. N. *J. Am. Chem. Soc.* **1993**, *115*, 10466–10467.
(25) Muller, F.; Arand, M.; Frank, H.; Seidel, A.; Hinz, W.; Winkler, L.; Hanel, K.; Blee, E.; Beetham, J. K.; Hammock, B. D.; Oesch, F *Eur. J. Biochem.* **1997**, *245*, 490–496.
(26) Franken, S. M.; Rozeboom, H. J.; Kalk, K. H.; Dijkstra, B. W *EMBO J.* **1991**, *10*, 1297–1302.
(27) Lu, A. Y. H.; Miwa, G. T. *Annu. Rev. Pharmacol. Toxicol.* **1980**, *20*, 513–531.
(28) Oesch, F. *Xenobiotica* **1972**, *3*, 305–340.
(29) Morisseau, C.; Hammock, B. D. *Annu. Rev. Pharmacol. Toxicol.* **2005**, *45*, 311–333.
(30) Kim, H. S.; Lee, O. K.; Hwang, S.; Kim, B. J.; Lee, E. Y. *Biotechnol. Lett.* **2008**, *30*, 127–133.
(31) Orru, R. V. A.; Faber, K. *Curr. Opin. Chem. Biol.* **1999**, *3*, 16–21.

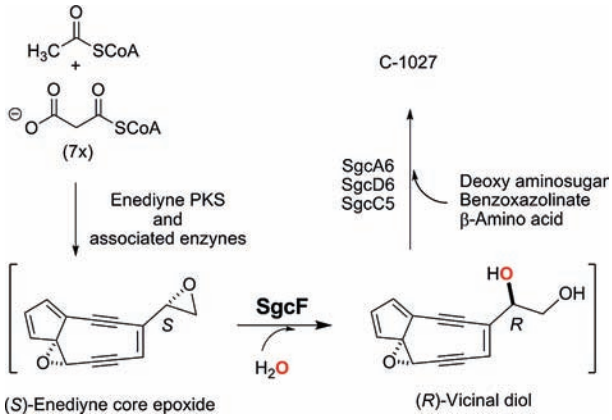

Figure 3. Proposed biosynthetic pathway for C-1027 involving an SgcF-catalyzed formation of a (*R*)-vicinal diol intermediate from a (*S*)-enediyne core epoxide precursor. The oxygen atom from water is shown in red.

and regioselective activities, whereby nucleophilic attack may occur at either epoxide carbon.

We have been studying the biosynthesis of the 9-membered enediynes C-1027, NCS, and maduropeptin as model systems to gain fundamental insight into the biochemical logic of enediyne biosynthesis. The biosynthetic gene clusters of each have been cloned, the involvement of which in enediyne biosynthesis has been confirmed by in vivo inactivation of selected genes within each cluster,[33−35] and in vivo and in vitro characterizations have unveiled numerous examples of unprecedented biochemistry and enzymology,[36−41] including a convergent biosynthetic strategy for this family of metabolites featuring vicinal diol intermediates (Figure 3). Sequence analysis indeed revealed one gene, *sgcF*, from the C-1027 biosynthetic gene cluster and two genes, *ncsF1* and *ncsF2*, from the NCS biosynthetic gene clusters, respectively, whose deduced gene products show high amino acid homology to known microbial EHs, including the Asp-His-Asp catalytic triad (Figure S2, Supporting Information). These findings are consistent with the proposed biosynthetic pathways, presenting outstanding opportunities to study the regio- and enantioselectivity of EHs involved in natural product biosynthesis.

Here we report the in vitro characterization of SgcF as an EH, supporting an (*R*)-vicinal diol as a key intermediate for C-1027 biosynthesis. SgcF efficiently catalyzes regio- and enantiospecific hydrolysis of (*S*)-styrene oxide, which serves as an enediyne core epoxide mimic, forming a covalent alkyl-enzyme intermediate at C-1 followed by hydrolysis to afford the (*R*)-phenyl vicinal diol exclusively. Interestingly, SgcF also hydrolyzes (*R*)-styrene oxide, albeit with significantly reduced efficiency, and regioselective formation of the monoester intermediate at the C-2 position also yields the (*R*)-phenyl vicinal diol as a preferred product. These data showed that SgcF catalyzes the net trans-addition of H_2O to (*S*)-styrene oxide in a Markovnikov manner but followed the opposite stereochemical course for (*R*)-styrene oxide in an anti-Markovnikov manner. Given the critical role EHs play in the biosynthesis of various natural products, including the enediynes, such enantioconvergence arising from complementary regioselective hydrolysis of a racemic substrate could be exploited to engineer epoxide hydrolases with improved regio- and/or enantiospecificity to increase natural product structural diversity.

Experimental Section

Strains, Plasmids and Cosmids. *Escherichia coli* DH5α and *E. coli* BL21(DE3) (Novagen, Madison, WI) were used as hosts for subcloning and heterologous expression, respectively, *E. coli* ET12567/pUZ8002 was used as the donor strain for conjugation,[42] and *Streptomyces globisporus* wild-type strain (C-1027-producing) has been described previously.[43] Plasmid pCDF-2 Ek/LIC was from Novagen, and pBS1005 was described previously.[43] SuperCos1 was from Stratagene (La Jolla, CA).

DNA Isolation and Manipulation. Plasmid preparation was carried out using commercial kits (Qiagen, Santa Clarita, CA). General procedures for DNA restriction digests, ligations and genetic manipulations in *E. coli* were performed according to standard protocols. *E. coli*-Streptomyces conjugation to introduce DNA into *S. globisporus* was performed according to the standard procedure[44] with the following modifications. *S. globisporus* spores were suspended in TSB medium and heat-shocked at 50 °C for 10 min, followed by incubation at 30 °C for 6 h. Germinated spores were mixed with *E. coli* ET12567/pUZ8002 cells and spread onto ISP4 plates freshly supplemented with 20 mM $MgCl_2$.

Chemicals and Instruments. Substrates including racemic styrene oxide, (*R*)-styrene oxide, and (*S*)-styrene oxide, products including racemic 1-phenyl-1,2-ethanediol, (*R*)-1-phenyl-1,2-ethanediol, and (*S*)-1-phenyl-1,2-ethanediol, and [^{18}O]-H_2O were purchased from Sigma-Aldrich (St. Louis, MO). Dithiothreitol (DTT) was purchased from Research Products International Corp (Mt. Prospect, IL). Complete protease inhibitor tablet, EDTA-free, was from Roche Applied Science (Indianapolis, IN). Medium components and buffers were from Fisher Scientific (Pittsburgh, PA). Synthetic DNA oligonucleotides were purchased from the University of Wisconsin-Madison Biotechnology Center (Madison, WI). PCR was performed with a PerkinElmer GeneAmp 2400. Electrospray ionization-mass spectroscopy (ESI-MS) was performed with an Agilent 1100 MSD SL ion trap mass spectrometer (Agilent Technologies, Inc. Santa Clara, CA). NMR spectra were recorded using a Varian UI-500 spectrometer (Varian, Inc., Palo Alto, CA). High performance liquid chromatography (HPLC) analyses were carried out on a Varian HPLC system equipped with Prostar 210 pumps, a photodiode array (PDA) detector, and an Alltech Appolo C18 reverse phase column (5 μm, 4.6 × 250 mm, Grace Davison Discovery Sciences, Deerfield, IL), using a 20 min linear gradient from 0 to 60% acetonitrile in H_2O. The enantiomeric separation was performed on a Waters HPLC system equipped with 600 pumps, a 996 PDA detector, and a Chiralcel OD-H chiral column

(32) Lee, E. Y. *Biotechnol. Lett.* 2008.
(33) Liu, W.; Christenson, S. D.; Standage, S.; Shen, B. *Science* **2002**, *297*, 1170–1173.
(34) Liu, W.; Nonaka, K.; Nie, L. P.; Zhang, J.; Christenson, S. D.; Bae, J.; Van Lanen, S. G.; Zazopoulos, E.; Farnet, C. M.; Yang, C. F.; Shen, B. *Chem. Biol.* **2005**, *12*, 293–302.
(35) Van Lanen, S. G.; Oh, T. J.; Liu, W.; Wendt-Pienkowski, E.; Shen, B. *J. Am. Chem. Soc.* **2007**, *129*, 13082–13094.
(36) Christenson, S. D.; Liu, W.; Toney, M. D.; Shen, B. *J. Am. Chem. Soc.* **2003**, *125*, 6062–6063.
(37) Lin, S.; Van Lanen, S. G.; Shen, B. *J. Am. Chem. Soc.* **2007**, *129*, 12432–12438.
(38) Lin, S. J.; Van Lanen, S. G.; Shen, B. *J. Am. Chem. Soc.* **2008**, *130*, 6616–6623.
(39) Lin, S. J.; Van Lanen, S. G.; Shen, B. *Proc. Natl. Acad. Sci. U.S.A.* **2009**, *106*, 4183–4188.
(40) Van Lanen, S. G.; Lin, S. J.; Shen, B. *Proc. Natl. Acad. Sci. U.S.A.* **2008**, *105*, 494–499.
(41) Zhang, J.; Van Lanen, S. G.; Ju, J. H.; Liu, W.; Dorrestein, P. C; Li, W. L.; Kelleher, N. L.; Shen, B. *Proc. Natl. Acad. Sci. U.S.A.* **2008**, *105*, 1460–1465.
(42) MacNeil, D. J.; Gewain, K. M.; Ruby, C. L.; Dezeny, G.; Gibbons, P. H.; MacNeil, T. *Gene* **1992**, *111*, 61–68.
(43) Liu, W.; Shen, B. *Antimicrob. Agents Chemother.* **2000**, *44*, 382–392.
(44) Kieser, T.; Bibb, M. J.; Buttner, M. M.; Chater, K. F.; Hopwood, D. A. *Practical Streptomyces Genetics*; The John Innes Foundation: Norwich, UK, 2000.

(5 μm, 4.6 × 250 mm, Grace Davison Discovery Sciences) using a 60 min isocratic elution with 2.5% isopropanol in n-hexane.

Inactivation of *sgcF*. The *sgcF* gene was inactivated by the λ-red mediated PCR-targeting method according to the literature protocol.[45] Since the backbone of pBS1005 is pOJ446,[43] which carries the replication origin of plasmid SCP2*, a 19-kb *Xba*I fragment from pBS1005 was subcloned into the same site of SuperCos1 to afford pBS1094. The apramycin (Apr) resistance gene *aac(3)IV*/*oriT* cassette was amplified by using the following pair of primers: *sgcF*F1: 5′-CGCGCCGCCCCGCTCCCACAATCACGAGGGTGGATTCACTATTCCGGGGATCCGTCGACC-3′/ *sgcF*R1: 5′-TCCGGCCGACGGGCGCTCCACTTCGTATGTGCCCTACTGGTTGTAGGCTGGAGCTGCTTC-3′ (underlined letters represent the oligonucleotide homologous to the flanking DNA regions of *sgcF*). The resulting PCR product was introduced into *E. coli* BW25113/pIJ790 harboring pBS1094 by electroporation, yielding the Δ*sgcF* mutated cosmid pBS1095 through λ-red mediated homologous recombination. Cosmid pBS1095 was then introduced into *S. globisporus* by *E. coli-Streptomyces* conjugation. Exconjugants that were apramycin resistant and kanamycin sensitive were selected as double crossover mutants and named SB1010, the genotype of which was confirmed by PCR using the following pair of primers: *sgcF*F1: 5′-CCGGGGACGGTCAATCTAG-3′/ *sgcF*R1: 5′-GCTCCCACAATCACGAGG-3′.

C-1027 Production, Isolation, and Analysis. Fermentation of *S. globisporus* wild-type and the Δ*sgcF* mutant strain SB1010 for C-1027 production was carried out using A9 medium as described previously.[46] Briefly, a spore suspension of the *S. globisporus* wild-type or recombinant strain was inoculated into 50 mL A9 medium in a 250 mL baffled flask and incubated at 28 °C, 250 rpm for 2 days. Five milliliters of the resultant seed culture was then used to inoculate 50 mL of A9 medium in 250 mL baffled flasks, and incubation continued at 28 °C, 250 rpm for 5 days. The culture was centrifuged (4000 rpm, 4 °C, 10 min) to collect the supernatant. This supernatant was first adjusted to pH 4.0 with 1 N HCl followed by centrifugation (4000 rpm, 4 °C, 8 min). The resultant supernatant was then added $(NH_4)_2SO_4$ to 70% saturation and readjusted to pH 4.0 to precipitate the C-1027 chromoprotein complex. The precipitated C-1027 chromoprotein complex was finally collected by centrifugation (4150 rpm, 4 °C, 20 min) and was extracted with acetone to isolate the C-1027 chromophore, which was subjected to HPLC analysis immediately.

The HPLC analysis was carried out on a C18 column (5 μm, 250 mm × 4.6 mm, Alltech, Lexington, KY). The column was equilibrated with 25% solvent A−75% solvent B and eluted with 25% solvent A−75% solvent B for 10 min followed by a linear gradient to 10% solvent A−90% solvent B in 15 min at a flow rate of 1 mL/min and with UV detection at 350 nm (solvent A, 10 mM phosphate buffer, pH 7.2 and solvent B, acetonitrile). Bioassay against *Micrococcus luteus* ATCC 9431 was performed as described.[43]

Cloning, Overproduction, and Purification of SgcF. The *sgcF* gene was amplified by PCR from cosmid pBS1005[33,43] using Platinum Pfx polymerase (Invitrogen, Carlsbad, CA) with the following primers: forward 5′-GAC GAC GAC AAG ATG CGT CCC TTC CGT ATC GA-3′ and reverse 5′-GAG GAG AAG CCC GG TCA GCG GAG CGG AGG GT-3′ (starting and stop codons underlined). The gel-purified PCR products were cloned into the pCDF-2 Ek/LIC vector using ligation-independent cloning as described by Novagen (Madison, WI) to give pBS1096 for *E. coli* expression. Overproduction in *E. coli* BL21 (DE3) and purification of SgcF by affinity chromatography using an NTA-Ni agarose column (Qiagen, Valencia, CA) were performed following the previously described procedure.[37,38] The purified SgcF was desalted using a PD-10 column (GE Healthcare, Piscataway, NJ) twice to completely remove glycerol, concentrated with a 10 K MWCO Vivaspin ultrafiltration device (Sartorius, Edgewood, NY), and stored at −80 °C in 100 μL aliquots. The purity of SgcF was assessed by SDS-PAGE on a 12% gel, and its concentration was determined from the absorbance at 280 nm using a molar absorptivity (ε = 96.9 mM^{-1} cm^{-1}) calculated using the program Protparam (http://www.expasy.ch/tools/protparam.html).

Activity Assay of SgcF. HPLC-based assays were carried out in 200-μL reaction mixture containing 2 mM racemic styrene oxide and 50 mM phosphate buffer (pH 7.5). The reaction was initiated by the addition of 100 μM SgcF and incubated at 28 °C for 90 min. The reaction was quenched by extracting with ethyl acetate (3 × 200 μL). After the solvent was removed using a speed-vac, the resulting residue was dissolved in 50 μL of acetonitrile, 25 μL of which was subjected to HPLC analysis. Control reactions were carried out under the identical conditions except with SgcF that had been boiled for 5 min.

To determine the kinetic parameters of SgcF-catalyzed hydrolysis of styrene oxide, a spectrophotometric assay method was adopted to achieve continuous and accurate determination of epoxide hydrolase activity.[47,48] Prior to kinetic analysis, the optimal pH for SgcF activity was tested in three different buffers—50 mM sodium acetate (pH 5.0, 5.5, and 6.0), 50 mM sodium phosphate buffer (pH 5.5 to pH 8.5), and 50 mM glycine-NaOH (pH 8.5, 9.0, and 10.0). The reactions were carried out in 1-mL reaction mixture containing 10 μL of 300 mM sodium periodate in DMF, 20 μL of 5 M styrene oxide in DMSO, and 50 mM buffer. The reactions were initiated by the addition of 10 μM SgcF and carried out in triplicate. The absorbance at 290 nm was monitored in a 1-mL quartz cell, and the velocity was calculated based on the rate of change of absorbance over several minutes. Steady-state kinetic parameters were obtained from reactions carried out in 50 mM phosphate buffer (pH 8.0) with varying styrene oxide concentrations [0.10 to 6.4 mM for (*S*)-styrene oxide and 1.0 to 24 mM for (*R*)-styrene oxide]. The assays were initiated by addition of SgcF [3.2 μM for (*S*)-styrene oxide and 9.6 μM for (*R*)-styrene oxide] and carried out in triplicate. The velocity was determined based on the change of the absorbance at 290 nm over several minutes. The Michaelis−Menten equation was fitted to plots of velocity of 1-phenyl-1,2-ethanediol formation versus substrate concentration to extract values for K_m and k_{cat}.

Large-Scale Reaction. To prepare sufficient quantities of product for NMR characterization, the reaction was carried out in 1-mL reaction mixture containing 10 mM styrene oxide and 200 μM SgcF in 50 mM phosphate buffer (pH 8.0). During the course of the reaction, 10 mM styrene oxide and 100 μM SgcF were added every hour. The reaction was allowed to proceed at 25 °C for 8 h, after which the products were extracted from the reaction mixture with ethyl acetate (5 × 0.5 mL). The solvent was removed by evaporation under reduced pressure. Purification by a flash column chromatography finally yielded the phenyl-1, 2-ethanediol product for NMR analysis and chiral analyses. [^{18}O]-labeled products were obtained following a similar procedure. The reactions were carried out in 0.5-mL reaction mixtures containing 80% [^{18}O]-H_2O. For (*S*)-styrene oxide, 5 mM substrate and 20 μM SgcF were added every 30 min. For (*R*)-styrene oxide, 20 mM substrate and 75 μM SgcF were added every hour.

Results

Bioinformatics Analysis. Close examination of the genes within the C-1027 biosynthetic gene cluster revealed a single gene, *sgcF*, whose deduced gene product showed high amino acid sequence homology to known microbial EHs.[33] Most EHs

(45) Gust, B.; Challis, G. L.; Fowler, K.; Kieser, T.; Chater, K. F. *Proc. Natl. Acad. Sci. U.S.A.* **2003**, *100*, 1541–1546.
(46) Van Lanen, S. G.; Dorrestein, P. C.; Christenson, S. D.; Liu, W.; Ju, J. H.; Kelleher, N. L.; Shen, B. *J. Am. Chem. Soc.* **2005**, *127*, 11594–11595.
(47) Doderer, K.; Lutz-Wahl, S.; Hauer, B.; Schmid, R. D. *Anal. Biochem.* **2003**, *321*, 131–134.
(48) Mateo, C.; Archelas, A.; Furstoss, R. *Anal. Biochem.* **2003**, *314*, 135–141.

belong to the $\alpha\beta$-hydrolase superfamily of proteins that share this common structural fold. SgcF contains several motifs that are conserved among this family of EHs: (i) the "nucleophilic elbow" motif Sm-X-Nu-X−Sm-Sm containing the Asp175 nucleophile (GGD^{175}WGK) that functions as a member of the nucleophile-His-acid catalytic triad (D^{175}, D^{336}, H^{363}); (ii) the oxyanion hole HGXP motif (HGW^{99}P); (iii) and the G-X-Sm-X-S/T motif[18,19,49] (G^{137}YGFS) that has been proposed to stabilize the interface between the lid and core domains,[18] and (iv) the conserved Tyr^{304} in helix 5 of the lid domain. Interestingly, the second Tyr in helix 1 of the lid domain (helix α4 in Figure S2, Supporting Information) has been changed to Trp^{236}. Taken together, the bioinformatic analysis predicts that SgcF is an EH responsible for the hydrolysis of an enediyne intermediate bearing an oxirane ring.

Inactivation of *sgcF*. The Δ*sgcF* mutant strain SB1010 completely lost its ability to produce C-1027. Inactivation of *sgcF* in *S. globisporus* was accomplished by following the λ-red-mediated PCR-targeting method to replace the entire *sgcF* gene with the *aac(3)IV/oriT* cassette, affording the Δ*sgcF* mutant strain SB1010 (Figure S3A and B, Supporting Information). Bioassays using *M. luteus* as a reference strain showed that the production of C-1027 was totally abolished in SB1010 either cultured on solid (ISP4) (Figure S3C, Supporting Information) or in liquid (A9) media (Figure S3D, Supporting Information). It was further confirmed by HPLC analysis that no C-1027 was produced by SB1010 when fermented in A9 media for 5 days (Figure S3E, Supporting Information), indicating that *sgcF* is indispensable for C-1027 biosynthesis.

Overproduction and Purification of SgcF. The *sgcF* gene was amplified from the cosmid pBS1005[33,43] and cloned into pCDF-2 Ek/LIC. After overproduction in *E. coli* BL21 (DE3), SgcF (~70 mg/L) was purified to homogeneity as an N-terminal His_6-tagged fusion protein using NTA-Ni affinity column chromatography. SDS-PAGE showed a single protein band consistent with the predicted molecular weight of SgcF (44.5 KDa) (Figure S4, Supporting Information).

Activity Assay for SgcF. Due to the unavailability of the oxirane-containing enediyne core that is predicted to be the substrate for SgcF, styrene oxide was chosen as a substrate mimic with which to test SgcF activity (Figure 3). The HPLC-based assay was carried out as described in the Experimental Section, and a single peak was eluted with a retention time identical to that of authentic 1-phenyl-1,2-ethanediol (Figure 4). The new peak was collected and analyzed by ESI-MS, yielding a $[M + Na]^+$ ion at *m/z* 161.2 (calcd $[M + Na]^+$ ion for molecular formula $C_8H_{10}O_2$ is 161.1). The absence of a styrene oxide peak in the HPLC chromatogram was attributed to its evaporation under reduced pressure, as indicated by the control experiments performed without enzyme.

Optimization of SgcF Activity. Prior to kinetic analysis, the pH dependence of SgcF-catalyzed hydrolysis was examined. The pH profile exhibited a bell-shaped curve between pH 6.0 to 10.0 with an optimal activity at pH 8.0 (Figure S5A, Supporting Information). As a result, all subsequent assays were performed in 50 mM phosphate buffer at pH 8.0. The reactions with different concentrations of SgcF showed that the SgcF-catalyzed hydrolysis of styrene oxide is enzyme-dependent (Figure S5B, Supporting Information).

Enantioselectivity of SgcF. Because most EH-catalyzed reactions exhibit stereo- and/or regio-selectivity, the enantioselectivity of SgcF was investigated using enantiomerically pure (*R*)- and (*S*)-styrene oxide substrates. A spectrophotometric assay was adopted to continuously monitor the formation of 1-phenyl-1,2-ethanediol,[47,48] thereby determining the steady-state kinetic constants for each enantiomer (Figure 5A and B). A plot of initial velocity versus the concentration of (*S*)-styrene oxide displayed Michaelis−Menten kinetics yielding a K_m of 0.6 ± 0.1 mM and k_{cat} of 48 ± 1 min^{-1}, while assays with variable (*R*)-styrene oxide gave a K_m of 2.0 ± 0.4 mM and k_{cat} of 4.3 ± 0.3 min^{-1}, respectively.

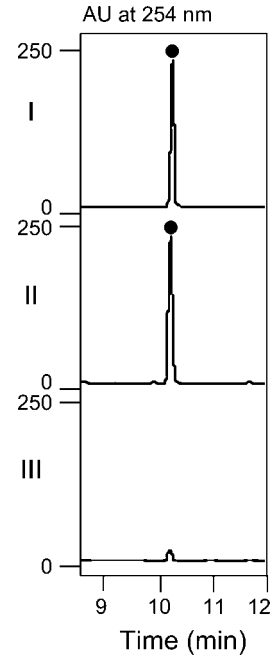

Figure 4. HPLC profiles for SgcF-catalyzed hydrolysis of racemic styrene oxide: (I) 1-phenyl-1,2-ethanediol standard; (II) with 100 μM SgcF for 90 min; and (III) with boiled SgcF for 90 min.

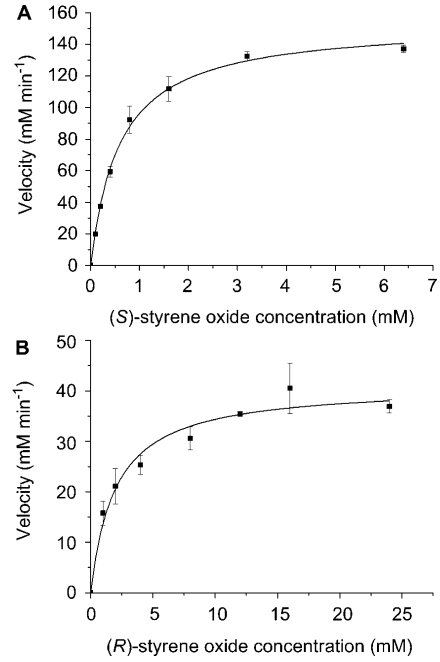

Figure 5. Kinetic analysis of SgcF-catalyzed hydrolysis of (*S*)- and (*R*)-styrene oxide showing single substrate kinetic plots for (A) (*S*)-styrene oxide and (B) (*R*)-styrene oxide.

(49) van Loo, B.; Kingma, J.; Arand, M.; Wubbolts, M. G.; Janssen, D. B. *Appl. Environ. Microb.* **2006**, *72*, 2905–2917.

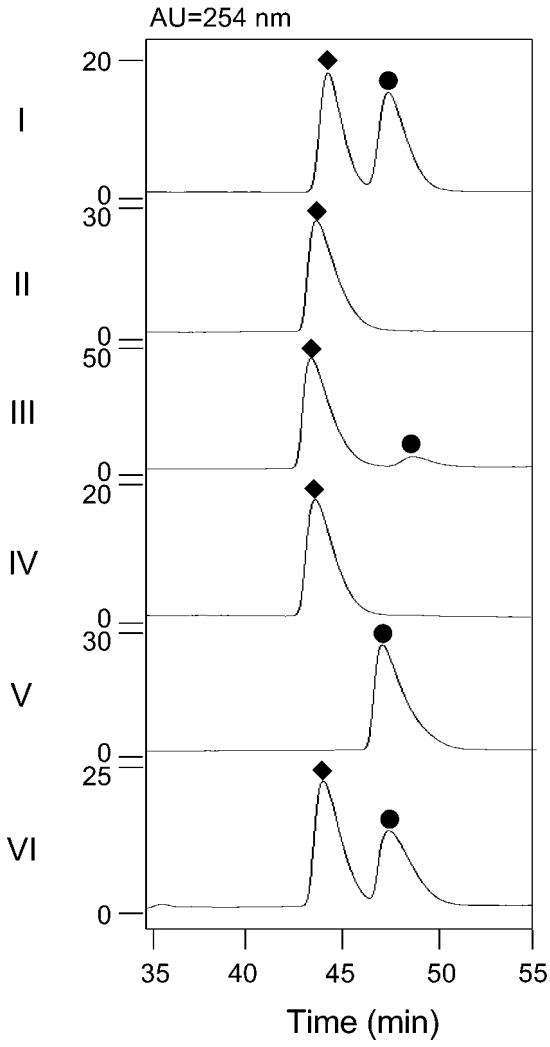

Figure 6. HPLC profiles for determination of the stereochemistry of 1-phenyl-1,2-ethanediol resulted from SgcF catalysis: (I) racemic 1-phenyl-1,2-ethanediol standard; (II) (*R*)-1-phenyl-1,2-ethanediol standard (◆); (III) SgcF-catalyzed hydrolysis of racemic styrene oxide; (IV) SgcF-catalyzed hydrolysis of (*S*)-styrene oxide; (V) (*S*)-1-phenyl-1,2-ethanediol standard (●); and (VI) SgcF-catalyzed hydrolysis of (*R*)-styrene oxide.

Thus, SgcF preferentially hydrolyzes (*S*)-styene oxide with a 37-fold greater specificity constant ($E = 37$), implicating an (*S*)-epoxide enediyne intermediate in C-1027 biosynthesis (Figure 3).

Stereochemistry of the Vicinal Diol Product. To determine the stereochemistry of the product, SgcF-catalyzed hydrolysis of racemic styrene oxide was performed on a large scale (1 mL) and the reaction was quenched by extraction of ethyl acetate when the reaction was complete as judged by thin layer chromotography. After ethyl acetate extraction and complete removal of solvent, ^{1}H NMR analysis in $CDCl_3$ confirmed the product as 1-phenyl-1,2-ethanediol by comparison to the authentic standard. Specifically, five protons at δ 7.3−7.4 ppm correspond to the hydrogens of the monosubstituted benzene ring, a doublet−doublet signal (δ 4.90 ppm, $J = 8.1$, 3.4 Hz) is associated with the proton at C-1, and two doublet−doublet signals (δ 3.83 ppm, $J = 11.5$, 3.4 Hz and δ 3.73 ppm, $J = 11.0$, 8.1 Hz) represent the two protons at C-2. Chiral HPLC analysis, however, revealed that (*R*)-1-phenyl-1,2-ethanediol was the dominant product (Panel III in Figure 6), a surprising finding given that no enantioselectivity would be expected if both

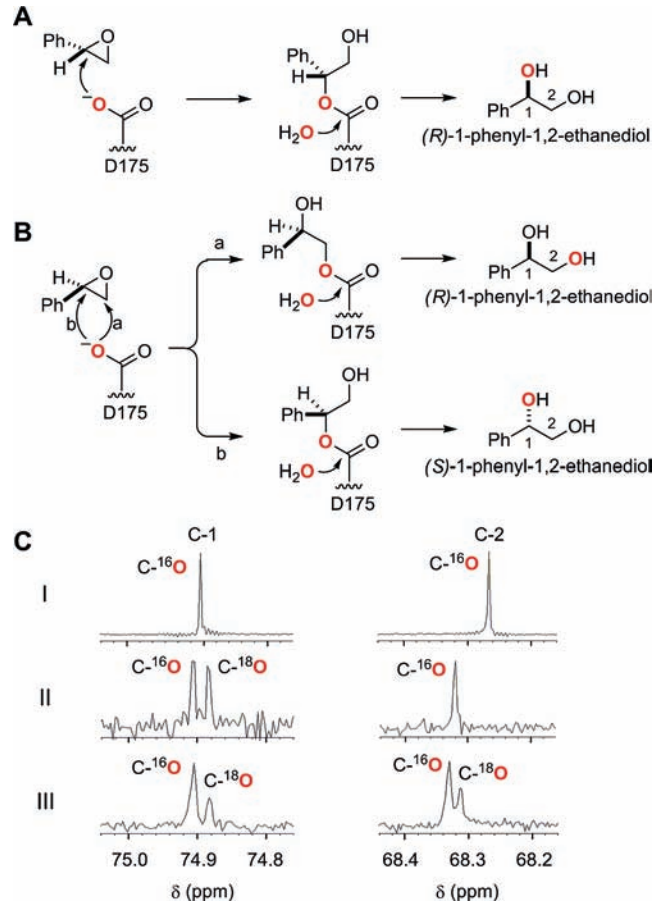

Figure 7. Regioselectivity of SgcF-catalyzed hydrolysis of (*S*)- and (*R*)-styrene oxide in [^{18}O]-H_2O: regioselective attack of the [^{18}O]-labeled (red) nucleophile Asp175 at (A) C-1 of (*S*)-styrene oxide and (B) C-1 and C-2 of (*R*)-styrene oxide, and (C) ^{13}C NMR spectra of C-1 and C-2 of 1-phenyl-1,2-ethanediol obtained from SgcF-catalyzed hydrolysis of (I) racemic styrene oxide in H_2O, (II) (*S*)-styrene oxide in [^{18}O]-H_2O, and (III) (*R*)-styrene oxide in [^{18}O]-H_2O.

epoxide enantiomers were hydrolyzed via the same mechanism (e.g., regioselective attack at the α-carbon). Consequently, the predominance of the (*R*)-vicinal diol product must arise from complementary stereo- and regioselective SgcF-catalyzed hydrolysis of each styrene oxide enantiomer. This intriguing finding prompted further investigation of this apparent enantioconvergent activity of SgcF.

Investigation of Enantioconvergent Mechanisms of SgcF-Catalyzed Hydrolysis. A few EHs have been reported to produce enantiomerically enriched diol products from racemic epoxides via complementary enantio- and regioselectivity.[30] The regioselectivity of the SgcF-catalyzed hydrolysis of (*S*)- and (*R*)-styrene oxide was investigated by performing the reaction for each individual enantiomer substrate in the presence of [^{18}O]-H_2O. ^{13}C NMR analysis of the resultant product from SgcF-catalyzed hydrolysis of (*S*)-styrene oxide showed a 2.8-Hz upfield shift that was exclusively associated with the C-1 position (Figure 7C), and chiral HPLC analysis confirmed the identity of the product as pure (*R*)-1-phenyl-1,2-ethanediol (Panel IV in Figure 6). This indicates a mechanism involving regiospecific nucleophilic attack at C-1 of (*S*)-styrene oxide (Figure 7A). By contrast, the product generated from (*R*)-styrene oxide revealed upfield shifts at both C-1 (2.8-Hz) and C-2 (2.4-Hz) (Figure 7C), and chiral HPLC analysis showed that (*R*)-

1-phenyl-1,2-ethanediol was produced with 20% ee (Panel VI in Figure 6). This labeling pattern is consistent with a lack of regiospecificity of the enzyme in attacking both C-1 and C-2 of (*R*)-styrene oxide (Figure 7B). These data establish that the enantiomerically enriched (*R*)-vicinal diol product from SgcF-catalyzed hydrolysis of racemic styrene oxide originates from complementary enantio- and regioselectivities of SgcF.

Discussion

C-1027, a chromoprotein antitumor antibiotic produced by *Steptomyces globisporus,* is composed of an apoprotein (CagA) and the C-1027 chromophore. The C-1027 chromophore consists of four distinct moieties - an enediyne core, a deoxy aminosugar, a benzoxazolinate, and an (*S*)-3-chloro-5-hydroxy-β-tyrosine moiety (Figure 1).[50−52] The 9-membered enediyne core readily undergoes Bergman cycloaromatization to generate a highly reactive diradical intermediate that abstracts hydrogen atoms from DNA, leading to both double-stranded breaks (DSBs) and interstrand cross-links (ICLs) that ultimately result in cell death.[53−55] Although the enediyne core directly confers cytotoxicity, the three peripheral moieties appended to the core are required for activity and stability. For instance, the benzoxazolinate moiety aids in binding to CagA that protects and carries the enediyne chromophore,[56,57] while the (*S*)-3-chloro-5-hydroxy-β-tyrosine also contributes critical binding interactions with CagA[58,59] and modulates the reactivity of the enediyne core via $\pi-\pi$ interactions.[59] A comparison of the biosynthetic gene clusters of C-1027,[33] NCS[34] and maduropeptin[35] suggested that these two moieties might be appended to a (*R*)-vicinal diol-containing C-1027 enediyne core, which in turn may originate from a (*S*)-enediyne core epoxide intermediate via EH-catalyzed ring-opening (Figure 3).

To test this hypothesis, we first carried out extensive bioinformatics analysis of the 56 genes within C-1027 biosynthetic gene cluster, and identified two genes, *sgcF* and *sgcI*, encoding α/β- hydrolases.[33] While bioinformatics analysis alone fell short of assigning SgcI as an EH, SgcF possesses such EH characteristics as the nucleophilic elbow (Sm-X-Nu-X−Sm-Sm), the G-X-Sm-X-S/T motif, the H-G-X-P oxyanion hole, and the Asp-His-Asp catalytic triad, and hence was annotated as an EH. Interestingly, SgcF contains only one of the two Tyr residues usually conserved in the lid domain (i.e., Y^{304}) that serve to activate the oxirane ring to nucleophilic attack, and the other is changed to Trp (i.e., W^{236}) (Figure S2, Supporting Information).[10,15−17,20−22,26] In vivo data showed that no C-1027 production was observed in the Δ*sgcF* mutant strain SB1010, unambiguously establishing that *sgcF* is indispensable for C-1027 biosynthesis. In vitro characterization of SgcF unveiled a canonical EH activity as demonstrated by the efficient hydrolysis of styrene oxide, a substrate mimic of the putative enediyne core epoxide (Figure 3). Specifically, SgcF efficiently hydrolyzes (*S*)-styrene oxide, displaying an apparent K_m of 0.6 ± 0.1 mM and k_{cat} of 48 ± 1 min^{-1}, via attack at the α-position to exclusively generate the (*R*)-phenyl vicinal diol, consistent with the stereochemistry of the C-1027 chromophore. These findings support the role of SgcF in the proposed convergent pathway for C-1027 biosynthesis, unveiling an (*R*)-vicinal diol as a key intermediate (Figures 1 and 3). Interestingly, SgcF can also hydrolyze (*R*)-styrene oxide to afford preferentially the (*R*)-phenyl vicinal diol via attack at the β-position, albeit with significantly reduced efficiency (apparent K_m of 2.0 ± 0.4 mM and k_{cat} = 4.3 ± 0.3 min^{-1}). However, the latter activity unlikely contributes to C-1027 biosynthesis in vivo since the oxygenase that catalyzes the formation of the enediyne core epoxide intermediate most probably would yield a single enediyne core epoxide, that is, the (*S*)-enantiomer, as a substrate for SgcF.

EHs are believed to be involved in the biosynthesis of a variety of natural products, including polyether antibiotics like nanchangmycin[60] and monensin,[61] plant cutin,[29] and insect pheromones.[62] The large diversity of putative EHs identified from genome sequences[49] implies that comparative studies may potentially reveal a great deal about the determinants of regio- and enantiospecificity of these enzymes. Indeed, comparative analyses of enediyne biosynthetic gene clusters[33−35] has predicted two EHs involved in the production of NCS - NcsF1 (53% identity to SgcF) and NcsF2 (62% identity to SgcF).[34] In a biosynthetic strategy that parallels SgcF, one would predict NcsF1 or NcsF2 to catalyze the hydrolysis of an (*R*)-enediyne core epoxide intermediate to afford an (*S*)-vicinal diol product for NCS biosynthesis (Figure 1). Comparative studies of SgcF and NcsF1 or F2 therefore would present a great opportunity to investigate how EHs evolve and acquire their exquisite regio- and enantioselectivity.

Most known EHs catalyze the hydrolysis of each enantiomer of a racemic mixture at a different rate to yield enantiomerically enriched vicinal diol products. However, this method of separation, or kinetic resolution, is limited by a maximum possible yield of 50%. In contrast, SgcF can not only catalyze the hydrolysis of (*S*)-styrene oxide to afford (*R*)-1-phenyl-1, 2-ethanediol exclusively but also hydrolyze (*R*)-styrene oxide to yield predominately (*R*)-1-phenyl-1, 2-ethanediol with 20% ee. Taken together, SgcF can generate (*R*)-1-phenyl-1, 2-ethanediol from racemic styrene epoxide with a minimal enantiomeric excess of 60% ee. SgcF therefore represents an excellent starting point for protein engineering efforts directed toward developing a biocatalyst for preparing enantiomerically pure diols from racemic epoxides.

In conclusion, the in vitro characterization of SgcF as an EH significantly advances our understanding of C-1027 biosynthesis,

(50) Hu, J.; Xue, Y. C.; Xie, M. Y.; Zhang, R.; Otani, T.; Minami, Y.; Yamada, Y.; Marunaka, T. *J. Antibiot.* **1988**, *41*, 1575–1579.
(51) Otani, T.; Minami, Y.; Marunaka, T.; Zhang, R.; Xie, M. Y. *J. Antibiot.* **1988**, *41*, 1580–1585.
(52) Otani, T.; Yasuhara, T.; Minami, Y.; Shimazu, T.; Zhang, R.; Xie, M. Y. *Agric. Biol. Chem.* **1991**, *55*, 407–417.
(53) Kennedy, D. R.; Gawron, L. S.; Ju, J. H.; Liu, W.; Shen, B.; Beerman, T. A. *Cancer Res.* **2007**, *67*, 773–781.
(54) Kennedy, D. R.; Ju, J.; Shen, B.; Beerman, T. A. *Proc. Natl. Acad. Sci. U.S.A.* **2007**, *104*, 17632–17637.
(55) Xu, Y. J.; Zhen, Y. S.; Goldberg, I. H. *Biochemistry* **1994**, *33*, 5947–5954.
(56) Matsumoto, T.; Okuno, Y.; Sugiura, Y. *Biochem. Biophys. Res. Commun.* **1993**, *195*, 659–666.
(57) Okuno, Y.; Otsuka, M.; Sugiura, Y. *J. Med. Chem.* **1994**, *37*, 2266–2273.
(58) Okuno, Y.; Iwashita, T.; Sugiura, Y. *J. Am. Chem. Soc.* **2000**, *122*, 6848–6854.
(59) Tanaka, T.; Fukuda-Ishisaka, S.; Hirama, M.; Otani, T. *J. Mol. Biol.* **2001**, *309*, 267–283.
(60) Sun, Y.; Zhou, X.; Dong, H.; Tu, G.; Wang, M.; Wang, B.; ZX, D. *Chem. Biol.* **2003**, *10*, 431–441.
(61) Gallimore, A.; Stark, C.; Bhatt, A.; Harvey, B.; Demydchuk, Y.; Bolanos-Garcia, V.; Fowler, D.; Staunton, J.; Leadlay, P.; Spencer, J. *Chem. Biol.* **2006**, *13*, 453–460.
(62) Abdel-Latief, M.; Garbe, L. A.; Koch, M.; Ruther, J. *Proc. Natl. Acad. Sci. U.S.A.* **2008**, *105*, 8914–8919.

supporting a (*R*)-vicinal diol as a key intermediate. The preference of SgcF for hydrolyzing (*S*)-styrene oxide to generate (*R*)-phenyl vicinal diol is consistent with the proposed convergent logic of C-1027 biosynthesis in which the benzoxazolinate and β-amino acid moieties are attached to an (*R*)-vicinal diol functionality of an (*S*)-enediyne core epoxide intermediate (Figure 3).[39,41] Furthermore, the complementary regioselectivity of SgcF, which leads to the enantioconvergent production of (*R*)-vicinal diol as the dominant product from a racemic epoxide, sets the stage to investigate the stereochemistry of EH catalysis and to engineer EHs with improved regio- and/or enantiospecificity.

Acknowledgment. We thank Dr. Y. Li, Institute of Medicinal Biotechnology, Chinese Academy of Medical Sciences, Beijing, China for the wild-type *S. globisporus* strain, the Analytical Instrumentation Center of the School of Pharmacy and Dr. Q. Cui, the National Magnetic Resonance Facility at UW-Madison for support in obtaining MS and NMR data, and Prof. W. Tang, School of Pharmacy, UW-Madison for the use of chiral HPLC. This work is supported in part by NIH grants CA78747 and CA113297. G.P.H. is the recipient of an NSERC postdoctoral fellowship.

Supporting Information Available: The structural model of AnEH (Figure S1), sequence alignment of SgcF (Figure S2), *sgcF* inactivation results (Figure S3), SDS-PAGE of purified recombinant SgcF (Figure S4), and pH (Figure S5A) and concentration (Figure S5B) dependence of SgcF. This material is available free of charge via the Internet at http://pubs.acs.org.

JA901242S